Risky business? Behavioral and neural mechanisms underlying risky decision-making in adolescents

Blankenstein, N.E.

Chapter 5

Individual differences in risk-taking tendencies modulate the neural processing of risky and ambiguous decision-making in adolescence

This chapter is published as: Blankenstein, N. E., Schreuders, E., Peper, J. S., Crone, E. A., & van Duijvenvoorde, A. C. K. (2018). Individual differences in risk-taking tendencies modulate the neural processing of risky and ambiguous decision-making in adolescence. *NeuroImage, 172, 663-673.*

Abstract

Although many neuroimaging studies have investigated adolescent risk taking, few studies have dissociated between decision-making under risk (known probabilities) and ambiguity (unknown probabilities). Furthermore, which brain regions are sensitive to individual differences in task-related and self-reported risk taking remains elusive. We presented 198 adolescents (11-24 years, an age-range in which individual differences in risk taking are prominent) with an fMRI paradigm that separated decision-making (choosing to gamble or not) and reward outcome processing (gains, no gains) under risky and ambiguous conditions, and related this to task-related and self-reported risk taking. We observed distinct neural mechanisms underlying risky and ambiguous gambling, with risk more prominently associated with activation in parietal cortex, and ambiguity more prominently with dorsolateral prefrontal cortex (PFC), as well as medial PFC during outcome processing. Individual differences in task-related risk taking were positively associated with ventral striatum activation in the decision phase, specifically for risk, and negatively associated with insula and dorsomedial PFC activation, specifically for ambiguity. Moreover, dorsolateral PFC activation in the outcome phase seemed a prominent marker for individual differences in task-related risk taking under ambiguity as well as self-reported daily-life risk taking, in which greater risk taking was associated with reduced activation in dorsolateral PFC. Together, this study demonstrates the importance of considering

multiple risk-taking measures, and contextual moderators, in understanding the neural mechanisms underlying adolescent risk taking.

Keywords: individual differences, risk taking, ambiguity, adolescence, fMRI

Introduction

Adolescence, defined as the developmental phase between childhood and adulthood, is often described as a period marked by increases in risky behaviors such as excessive alcohol use and reckless driving, and a strong need for exploration (Crone & Dahl, 2012; Steinberg, 2008). Theoretical models have explained this rise in risk-taking behavior by long-lasting development of subcortical and cortical brain regions and their connections, in which regions involved in affective processing and reward sensitivity peak in reactivity during adolescence, whereas cortical brain regions supporting cognitive control undergo a more protracted development (Casey, Jones, & Hare, 2008; Somerville, Hare, & Casey, 2011; Crone & Dahl 2012; Casey 2015). Although a wealth of research has focused on the neural mechanisms underlying adolescent risk taking, few studies have systematically investigated the relation with actual risk-taking behavior either inside or outside the laboratory. These studies report conflicting findings, have relatively small sample sizes, or focus on only one or two brain regions-of-interest (for an excellent review, see Sherman, Steinberg, & Chein, 2017). Furthermore, although adolescence may be a period of heightened risk-taking tendencies on average, not all adolescents are risk takers (Bjork & Pardini, 2015), and risk-taking tendencies vary substantially between adolescents. Thus, including predictors of behavior on the individual level may be key in understanding what drives adolescent risk taking. In this study we investigated the neural mechanisms underlying individual differences in adolescent risk taking, using task-related and self-report measures of risk-taking tendencies in a large adolescent sample.

A number of brain regions have been associated with individual differences in risk-taking tendencies in adolescence (Sherman et al., 2017). For instance, a greater ventral striatum (VS) response when receiving monetary rewards has been associated with a greater self-reported drive to pursuit rewards, fun-seeking tendencies (Braams, van Duijvenvoorde, Peper, & Crone, 2015; Van Duijvenvoorde et al., 2014), the likelihood of engaging in real-life risky behaviors (Galvan, Hare, Voss, Glover, & Casey, 2007), and increased frequencies of illicit drug use, binge drinking, and sexual risky behaviors (Bjork & Pardini, 2015; Braams, Peper, van der Heide, Peters, & Crone, 2016). The ventromedial prefrontal cortex (VMPFC),

closely interacting with the VS, has been additionally related to measures of reward sensitivity in adolescents (Van Duijvenvoorde et al., 2015) as well as with greater risk preferences in adults (Blankenstein, Peper, Crone, & Duijvenvoorde, 2017; Engelmann & Tamir, 2009). Conversely, reduced risk-taking tendencies in laboratory choice tasks have been related to increased anterior insula and dorsomedial prefrontal cortex (DMPFC) activation, regions that are typically related to conflict and uncertainty in decision making, and to the integration of cognitive and affective neural signals (Smith, Steinberg, & Chein, 2014; Van Duijvenvoorde et al., 2015; Van Leijenhorst et al., 2010). Finally, reduced activation in the lateral prefrontal cortex (LPFC), a key region involved in self-control (Dixon, 2015), has been associated with greater laboratory risk taking in young adults (Gianotti et al., 2009). In contrast, studies with adolescents have shown that longitudinal declines in LPFC activation were associated with declines in self-reported frequency of real-life risky behaviors (such as getting high or drunk at parties; Qu, Galvan, Fuligni, Lieberman, & Telzer, 2015). Taken together, these studies highlight candidate regions sensitive to individual differences in risk-taking tendencies, yet none of these studies have included a substantial adolescent sample size, nor provided a comprehensive overview of task-related, and self-reported, measures of risk taking.

Importantly, the majority of these studies used fMRI paradigms that present explicit risky (e.g., the Columbia Card Task; Van Duijvenvoorde et al., 2015), rather than ambiguous risky, choice contexts. That is, while explicit risk presents known probabilities (such as in a coin toss, in which the chance of 'tails' is known: 50%), ambiguity presents unknown probabilities (such as texting while driving: the chance of causing an accident, for example, is unknown; Tversky & Kahneman, 1992). However, the majority of risky situations in daily life presents ambiguous risk. Indeed, in adolescence, the tendency to gamble under ambiguity, but not risk, has been associated with individual differences in real-life risk-taking behavior, such that a higher 'tolerance' to ambiguity was related to higher levels of reckless behavior such as speeding and having unprotected sex (Blankenstein, Crone, van den Bos, & van Duijvenvoorde, 2016; Tymula et al., 2012), and rebellious behavior such as staying out late (van den Bos & Hertwig, 2017). This may suggest that behavior under ambiguity is a better reflection of adolescent risk taking in real life (Blankenstein et al., 2016; Tymula et al., 2012; van den Bos & Hertwig, 2017). Possibly, a tolerance to ambiguity in adolescence is important for accomplishing important goals prominent in adolescence, such as exploring new environments, and gathering information about the world (e.g., Crone & Dahl, 2012; Hartley, & Somerville, 2015). Consequently, distinguishing the mechanisms underlying risk and ambiguity coding in adolescence is pivotal given that these may have different relations with observed risk-taking

behavior in adolescence. To date, the neural mechanisms underlying risky versus ambiguous decision-making have not been investigated in adolescence, nor have these been related to individual differences in risk-taking tendencies in adolescence.

Taken together, we aimed to elucidate individual differences in task-related and self-reported risk-taking behavior in relation to brain activation in risky and ambiguous decision contexts, in 198 adolescents aged 11 to 24 years, an age range in which individual differences in daily-life risk taking are most prominent (Bjork & Pardini, 2015; Willoughby, Good, Adachi, Hamza, & Tavernier, 2013). We applied the same paradigm as has been previously reported in a different sample of young adults (Blankenstein et al., 2017), which allows to study choice (choosing to gamble or not) and reward processing (gains versus no gains) under risk and ambiguity. In line with this prior study with adults, we expected few overall differences between risky and ambiguous gambling (Blankenstein et al., 2017, but see Hsu, Bhatt, Adolphs, Tranel, & Camerer, 2005; Huettel, Stowe, Gordon, Warner, & Platt, 2006), although we expected that the DMPFC would particularly distinguish between risky and ambiguous outcomes (Blankenstein et al., 2017). Particularly, we expected that individual differences in risk-taking tendencies would be positively associated with activation in VS and VMPFC, and negatively with DMPFC, insula, and LPFC. Given the mixed findings on the LPFC, this relation could also be reversed (i.e., enhanced activation with greater risk taking; Qu et al., 2015; Telzer, Fuligni, Lieberman, & Galván, 2013). Second, given that behavior under ambiguity, but not risk, has been related to real-life risk-taking tendencies (Blankenstein et al., 2016; Tymula et al., 2012; van den Bos & Hertwig, 2017), we expected these brain-behavior associations to be more pronounced under conditions of ambiguity than risk.

Methods

Participants

Two hundred and sixteen right-handed individuals (110 females, 106 males) between 11 and 24 years old participated in this study. Participants were part of a longitudinal study ('Braintime', which included three time points each separated by a two-year interval), and were recruited through schools and local advertisements. The data of the current study were collected at the third time point, and this was the first time the current task was presented. Eighteen participants were excluded from analyses because they were either diagnosed with a psychiatric disorder (n = 5), exceeded movement in the MRI scanner with more than 3 mm (n = 1), loss of data (n = 3), or because of too few trials in which the gambling option was chosen

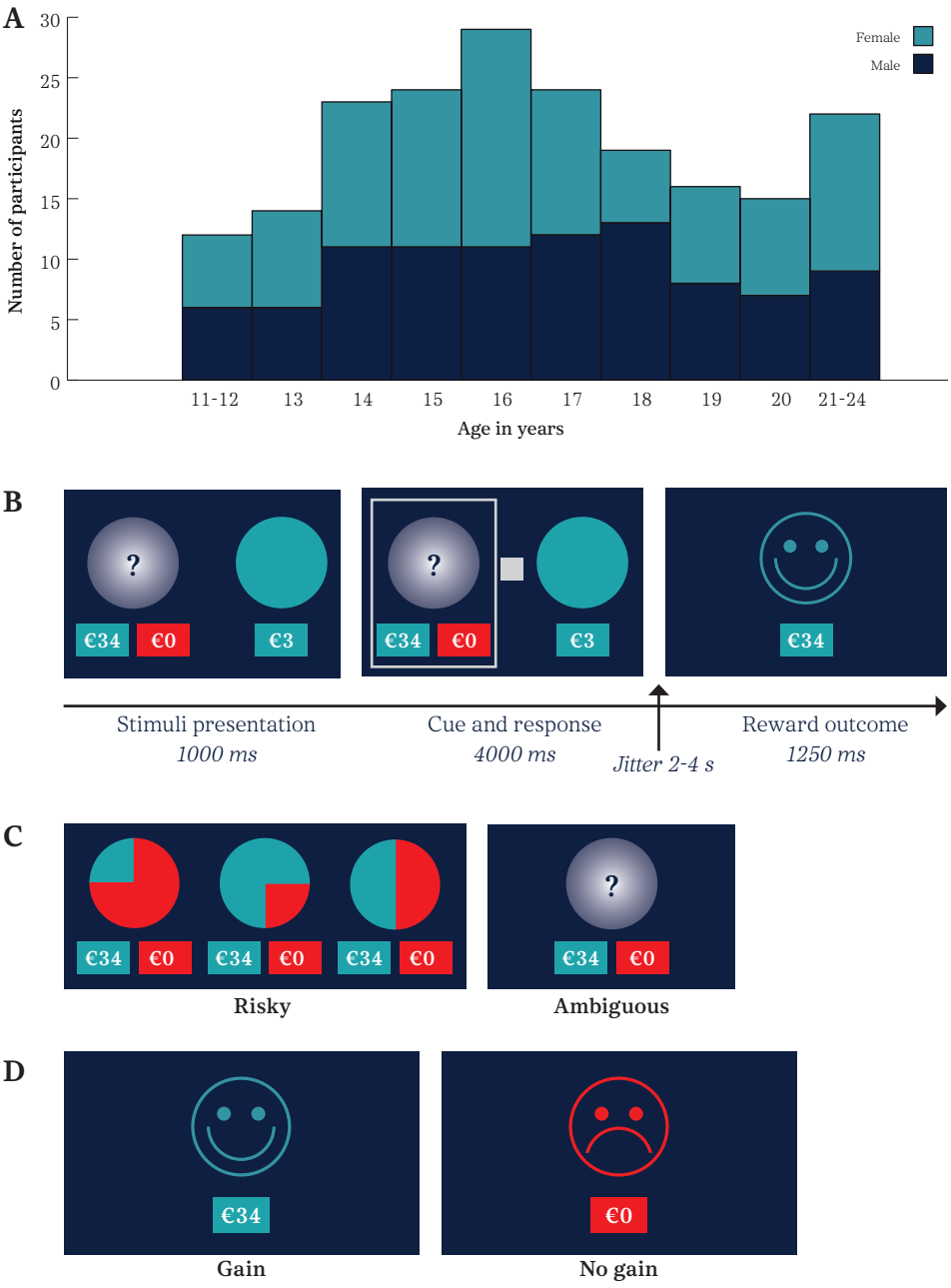

Figure 1. A. *Number of participants across age per gender.* ***B.*** *Example trial of the wheel of fortune task showing an ambiguous trial with gain as reward outcome.* ***C.*** *The different gambling wheels.* ***D.*** *Gain and no gain outcomes.*

(i.e., fewer than five gambles in either the risky or ambiguous condition, n = 9; see 'Wheel of fortune task'). The final sample therefore included 198 healthy participants (94 female, 104 male, M_{Age} = 17.15, SD_{Age} = 2.75, range 11.94 – 24.68 years, see Figure 1A). IQ fell in the normal range, as estimated on previous time points of the longitudinal Braintime study (T1: M = 110.08, SD = 9.54; T2: M = 107.84, SD = 10.17), using subtests of the WISC-III (participants 8- to 15-years old) or WAIS-III (participants 16 and older), and did not correlate with age (see also Braams et al., 2015; Peters, Van Duijvenvoorde, Koolschijn, & Crone, 2016).

This study was approved by the institutional review board of the University Medical Center. Adult participants and parents of underage participants provided written informed consent, and underage participants provided written assent. All anatomical scans were cleared by a radiologist and no abnormalities were reported. Participants were screened for MRI contra indications and psychiatric or neurological disorders and had normal or corrected-to-normal vision.

Wheel of fortune task

Participants played a child-friendly wheel of fortune task (see Figure 1 and Blankenstein et al., 2017). Participants made a series of choices between pairs of wheels. One wheel represented a safe option (i.e., a 100% chance of winning 3 Euro), whereas the other option represented a gambling option which could yield more money (i.e., €31, €32, €33, or €34) but could also yield nothing (€0). The gambling option could either be risky (probabilities were known) or ambiguous (probabilities were unknown), and the safe option was a sure gain of €3 on every trial. In the risky wheels, gain probabilities were presented as the portions of the wheels in blue, whereas no gain probabilities were presented as the portions of the wheel in red. Of the risky trials, 30 trials reflected a gamble with a 50% gain probability, 8 trials reflected a gamble with a 75% gain probability, and 8 trials reflected a gamble with a 25% gain probability (Figure 1C). In the ambiguous trials, the wheel was covered with a grey lid showing a question mark (Figure 1C). Participants played 46 ambiguous trials and 46 risky trials, which were presented inter-mixed.

After the choice, participants were presented with the reward outcome (Figure 1D; gain, no gain). The task was programmed such that the probabilities presented in the wheels (25%, 50%, and 75%) matched the actual probabilities of winning when choosing the gambling option. That is, when presented with a 75% risky trial, there was a 75% chance of winning when choosing to gamble. Furthermore, the order of gains and no gains was randomized for each participant, and the computer randomly (without replacement) selected one of the four possible amounts (€31, €32, €33, or €34) to present on a trial-by-trial basis. The outcome for gains was

presented with the amount in blue over a smiley face, and the outcome for no gains was presented with €0 in red over a sad face. Finally, the expected value (i.e., the probability*amount) of the gambling options was much higher than the safe option (which was consistently €3). This was done to encourage gambling behavior, so that participants had a sufficient number of trials for the comparisons of brain activation of gambling under risk and under ambiguity, their corresponding reward outcomes, and associations with individual differences in risk-taking tendencies.

The task was presented in the scanner via E-prime (Psychology Software Tools). Participants were presented with the pairs of wheels presenting a gamble and safe option. Gamble and safe options were randomly displayed on the left or right side of the screen on a trial-by-trial basis. After 1000 msec a grey square appeared in the center of the screen, prompting the participants to respond. A response had to be given within a 3000 msec interval. Participants responded with their right index finger (to select the wheel on the left) and right middle finger (to select the wheel on the right). A grey selection frame around the chosen wheel confirmed the response, and remained visible for the duration of the 3000 msec interval. If participants failed to respond within 3000 msec, the words 'TOO LATE' appeared in the center of the screen for 1250 ms, after which the next trial began. On average, 0.99% of the trials did not include a response, and these trials were excluded from all analyses. The choice phase was separated from the outcome phase by a fixation cross of 2-4 seconds (jittered, with increments of 500 msec). The reward outcomes (gain, no gain, or safe gain) were presented for 1250 msec. The inter-trial-intervals and the optimal trial sequence were determined with OptSeq (Dale, 1999), with jittered intervals varying between 0 and 9350 ms. In addition, each trial was preceded by a 500 ms fixation cross, which was not part of the inter-trial-interval.

Questionnaires

To test for associations between brain activation during decision-making under risk and ambiguity and indices of real-life risk taking, 192 participants completed the Adolescent Risk-Taking Questionnaire (ARQ; Gullone, Moore, Moss, & Boyd, 2000). In particular, we focused on the *behavior* scale of this questionnaire, which assesses the frequency of engaging in risky activities in real life with four subscales: Thrill-seeking (Cronbach's α = .205), Rebellious (α = .888), Reckless (α = .497), and Antisocial behavior (α = .508). Participants indicated on a 5-point Likert scale how often they engaged in risky activities (with 1 indicating *never* and 5 indicating *very often*). Examples include 'Snow skiing' (Thrill-seeking), 'Staying out late' (Rebellious), 'Having unprotected sex' (Reckless), and 'Cheating' (Antisocial).

To test for associations with self-reported reward approach and avoidant

behavior, 182 participants completed the Behavioral Inhibition System/Behavioral Activation System questionnaire (BIS/BAS; Carver & White, 1994). The BIS/BAS questionnaire is comprised of four subscales: BAS Drive (a measure of persistence in the pursuit of goals, α = .750), BAS Fun seeking (a measure of desire for rewards and the willingness to approach rewards, α = .512), BAS Reward Responsiveness (a measure of responses to rewards and reward anticipation, α = .659), and BIS (a measure of punishment sensitivity, α = .779). Participants indicated on a 4-point Likert scale the degree to which statements were applicable to them with (with 1 indicating *very true* and 4 indicating *very false*). Examples include 'When I want something I usually go all-out to get it' (BAS Drive), 'I'm always willing to try something new if I think it will be fun' (BAS Fun seeking), 'When I get something I want, I feel excited and energized' (BAS Reward responsiveness), and 'I worry about making mistakes' (BIS). Items were recoded such that higher scores indicates more approach (BAS) or avoidant (BIS) behavior.

Procedure

Participants received instructions about the MRI session in a quiet laboratory room, and were accustomed to the MRI environment with a mock scanner. Next participants received instructions about the wheel of fortune task, and practiced ten trials on a laptop. We explained to the participants that the ambiguous wheel could reflect a gamble of any of the risky probabilities (i.e., 25%, 50%, 75%). In addition, we explained that the computer would randomly select the outcomes of three trials, of which the average amount was paid out in addition to the standard payout fee. Eventually, the computer selectively drew a gain, a no gain, and a safe gain outcome (or a gain and two no gain outcomes if the participant never chose the safe option). This draw amounted to an additional rounded payout of €11 or €12 for each participant.

The wheel of fortune task lasted approximately 18 minutes, in two runs of 9 minutes each, win a short break in between. Participants could respond with their right index and middle fingers using a button box that was attached to the participant's leg. The task was followed by a high-definition structural scan, which lasted approximately five minutes.

Participants completed the ARQ and BIS/BAS questionnaire at home, online via Qualtrics (www.qualtrics.com), before the scan date. Adult participants received €60 and underage participants received €30 for their participation, in addition to their winnings in the wheel of fortune task (€11 or €12), and small presents.

MRI data acquisition

We used a 3T Philips scanner (Philips Achieva TX) with a standard whole-head coil. Functional scans were acquired during two runs of 246 dynamics each, using T2* echo-planar imaging (EPI). The volumes covered the whole brain (repetition time (TR) = 2.2 s; echo time (TE) = 30 ms; sequential acquisition, 38 slices; voxel size 2.75 x 2.75 x 2.75 mm; field of view (FOV) = 220 x 220 x 114.68 mm). The first two volumes were discarded to allow for equilibration of T1 saturation effects. A high-resolution 3D T1 scan for anatomical reference was obtained after the wheel of fortune task (TR = 9.76 msec, TE = 4.59 msec, 140 slices, voxel size = 0.875 mm, FOV = 224 × 177 × 168 mm).

MRI data analyses

Preprocessing

We analyzed the data with SPM8 (Wellcome Department of Cognitive Neurology, London). Images were corrected for slice timing acquisition and rigid body motion. Functional volumes were spatially normalized to T1 templates. Translational movement parameters never exceeded 3 mm (< 1 voxel) in any direction for any participant or scan (movement range: 0.31 – 0.19 mm, M = 0.065, SD = 0.028). The normalization algorithm used a 12-parameter affine transform with a nonlinear transformation involving cosine basis function, and resampled the volumes to 3 mm^3 voxels. Templates were based on MNI305 stereotaxic space. The functional volumes were spatially smoothed using a 6 mm full width at half maximum (FWHM) isotropic Gaussian kernel.

General-Linear model

We used the general linear model (GLM) in SPM8 to perform statistical analyses on individual participants' data. The fMRI time series were modeled as a series of two events convolved with a canonical hemodynamic response function (HRF): the choice phase and the outcome phase. First, the onset of the choice phase was modeled with a duration of response (1000 msec + response time; see Figure 1). Events were modeled separately for gambling under risk and gambling under ambiguity, and for choosing the safe option under risk and choosing the safe option under ambiguity, which resulted in four conditions: Risk Gamble, Ambiguity Gamble, Risk Safe, and Ambiguity Safe. Second, the onset of the outcome phase was modeled with zero duration. We modeled the outcomes (gain, no gain, and safe gain) following a risky or ambiguous gamble, or safe choice, which resulted in six conditions in the outcome phase: Risk Gain, Risk No Gain, Ambiguity Gain, Ambiguity No Gain, Risk Gain Safe, and Ambiguity Gain Safe. In the current study we were particularly interested

in brain activation during gambling, and brain activation during reward processing following a gamble.

Trials on which participants did not respond were modeled separately as a covariate of no interest. In addition, we included six motion parameters as noise regressors. The least-squares parameter estimates of the height of the best-fitting canonical HRF for each condition separately were used in pairwise contrasts. These pairwise comparisons resulted in subject-specific contrast images, which were used for the second-level group analyses. We conducted all second-level group and regression analyses with Family Wise Error (FWE) cluster correction ($p < .05$, using a primary voxel-wise threshold of $p < .001$, uncorrected; Blankenstein et al., 2017; Woo, Krishnan, & Wager, 2014). We used the MarsBaR toolbox (Brett, Anton, Valabregue, & Poline, 2002; http://marsbar.sourceforge.net) to visualize patterns of activation in clusters identified in the whole-brain regressions. Finally, the coordinates of local maxima are reported in MNI space.

Analyses with individual differences

First, we included a GLM to test for associations between brain activation and individual differences in gambling behavior in the wheel of fortune task (i.e., task-related risk-taking tendencies). A second model was included to test for associations with ARQ and BIS/BAS scores (i.e., self-reported risk-taking tendencies). Task-related risky and ambiguous gambling were both included in the first model so that when testing for unique effects of risky gambling, we controlled for ambiguous gambling (i.e., this was a covariate of no interest), and vice versa. The same approach was used for the ARQ and BIS/BAS questionnaire, in which we entered all subscales of both questionnaires in one model. Due to the absence of correlations between task behavior and self-report measures, including all individual-difference measures in one GLM did not change any of the reported findings. Finally, although age was not included as a regressor of interest in our primary models, we ran our models with and without age (linear) as a covariate, and report in the text which results remain significant when controlling for age. In addition, we exploratively report effects of age in the corresponding tables.

Results

Behavioral results

Table 1 summarizes the correlations between the behavioral measures (wheel of fortune task, ARQ, and BIS/BAS). In the wheel of fortune task (n = 198), a paired samples t-test showed that participants gambled a comparable proportion of times under risk and under ambiguity ($t(197)$ = -.158, p = .116, M_{risk} = .74, SD_{risk} = .21, $range_{risk}$ = .22 – 1.00, M_{ambig} = .76, SD_{ambig} = .25, $range_{ambig}$ = .11– 1.00), although there were individual differences in gambling behavior (see Figure 2A). A correlation analysis showed that gambling under risk and ambiguity were correlated (r = .686, p < .001; Table 1). Furthermore, a paired samples t-test on reaction times showed that when choosing to gamble, participants responded significantly slower in ambiguous than in risky trials ($t(197)$ = -5.41, p < .001, M_{risk} = 585.81, SD_{risk} = 193.51, M_{ambig} = 645.36, SD_{ambig} = 213.63). Finally, given the presence of outcome feedback in the task, we tested for changes in behavior under risk and ambiguity across time. To this end, we divided gambling behavior across four task bins of 11 or 12 trials per bin, per condition (risk and ambiguity). A within (task bin) * between (risk vs ambiguity) subjects ANOVA with age as a covariate showed a significant interaction effect between condition and task bin ($F(3, 576)$ = 5.84, p < .001, η^2 = .03; Figure 2B), in which gambling increased slightly across task bins in the ambiguous ($F(3, 579)$ = 18.83, p < .001, η_p^2 = .09) but not in the risky condition ($F(3, 579)$ = 1.11, p = .35).

Correlation analyses on the ARQ questionnaire (n= 192) showed that the subscales were all moderately correlated, with the exception of Thrill-seeking and Rebellious behavior (Table 1). With respect to the BIS/BAS questionnaire (n = 182), we observed that BAS Drive, BAS Fun seeking, and BAS Reward responsiveness were moderately correlated, and that BAS Reward responsiveness was additionally correlated with BIS. Furthermore, correlation analyses between the ARQ and BIS/BAS scores (n = 179) showed that ARQ Rebellious was correlated with BAS Drive and BAS Fun seeking, and that ARQ Reckless and ARQ Antisocial were both correlated with all BAS subscales. Finally, task behavior was not related to any of the self-report measures (Table 1). Age effects on all behavioral measures are reported in the supplementary materials (Appendix A1).

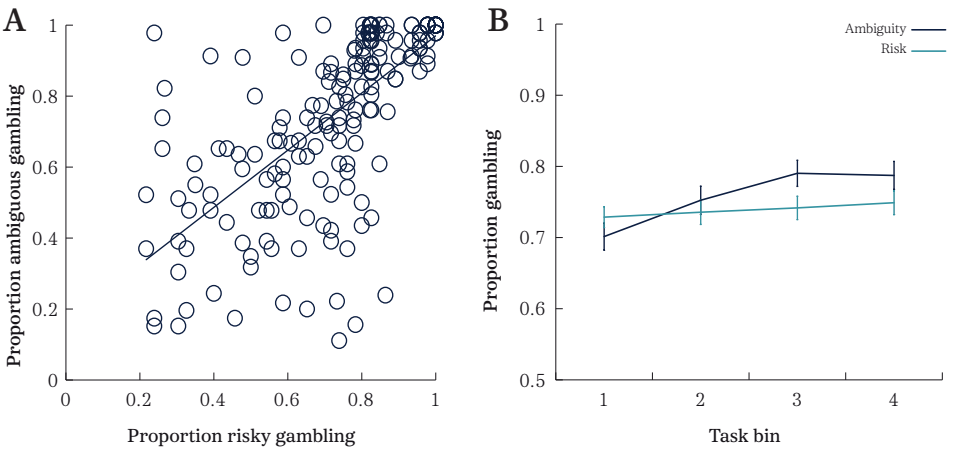

Figure 2. A. *Correlation between proportion gambling under risk and proportion gambling under ambiguity in the wheel of fortune task.* ***B.*** *Proportion gambling across time (task bins) for the ambiguous (black line) and risky (grey line) conditions. The y-axis is displayed from 0.5 to 1 to more clearly illustrate the interaction effect.*

Table 1. Correlation matrix of the behavioral measures, showing Pearson's *r*.

		1	2	3	4	5	6	7	8	9	10
1	Risky gambling	–									
2	Ambiguous gambling	**.686**$^{***\circ}$	–								
3	ARQ Thrill-seeking	-.050	-.006	–							
4	ARQ Rebellious	.115	.043	.092	–						
5	ARQ Reckless	.114	.064	**.144***	**.486**$^{***\circ}$	–					
6	ARQ Antisocial	.064	-.019	**.206****	**.479**$^{***\circ}$	**.275**$^{***\circ}$	–				
7	BAS Drive	.079	.094	.090	**.206****	**.185***	**.197****	–			
8	BAS Fun seeking	.069	.132	.171*	**.383**$^{***\circ}$	**.240****	**.259**$^{***\circ}$	**.485**$^{***\circ}$	–		
9	BAS Reward responsiveness	.002	.064	.086	.122	**.180***	**.163***	**.414****	**.415**$^{***\circ}$	–	
10	BIS	.069	-.008	-.135	.048	-.050	.086	-.008	-.103	**.270**$^{***\circ}$	–

*Note. Risky and ambiguous gambling: n = 198, ARQ: n = 192, BIS/BAS: n = 182, ARQ and BIS/BAS: n = 179. ° Correlation is significant with Bonferroni correction for multiple comparisons ***Correlation is significant at p < .001 (two-tailed, uncorrected for multiple comparisons). **Correlation is significant at p < .01 (two-tailed, uncorrected for multiple comparisons). *Correlation is significant at p < .05 (two-tailed, uncorrected for multiple comparisons).*

fMRI results

Whole-brain contrasts

Choice phase - First, we investigated which brain regions showed greater activation during gambling under risk versus ambiguity. The contrast Risk Gamble > Ambiguity Gamble revealed greater activation for risk compared to ambiguity in the bilateral precentral gyrus, right VLPFC, and posterior parietal cortex (PPC; Figure 3A, Table 2). The reversed contrast (Ambiguity Gamble > Risk Gamble) resulted in left DLPFC, bilateral temporal lobe, inferior parietal cortex (angular gyrus) and precuneus activation (Figure 3B, Table 2). When exploratively testing for effects of age, only activation in the superior parietal lobe increased with age for gambling under ambiguity compared with risk (see Table A1; Figure A1.E).

Although in the current study we were interested in contrasting risky and ambiguous gambling, an additional interesting analysis may be to compare gambling versus choosing safe across risk and ambiguity. We report the results of this analysis in the supplementary materials (Appendix A2; Table A2; Figure A1.A-D).

Outcome phase - To test which regions coded reward outcomes, we first calculated the contrast Gain > No Gain. This contrast resulted in robust activation in bilateral striatum, VMPFC, PPC, and angular gyrus (Figure 3C, Table 4). When exploring age effects on this contrast, we observed greater superior parietal and motor cortex activation for younger ages (Table A3; Figure A1.F).

To more specifically examine which regions differentially coded reward outcomes following a risky versus ambiguous gamble, we ran a whole-brain condition (risk, ambiguity) * reward outcome (gain, no gain) ANOVA. This resulted in a significant interaction effect in the MPFC (Figure 3D; Table 4). To understand the direction of this interaction effect, we plotted the parameter estimates of this region for risk and ambiguity, and gain and no gain, separately (Figure 3D, right panel). From this plot it can be seen that this interaction is particularly driven by reward outcomes following an ambiguous gamble. That is, the difference in brain activation in the MPFC between gain and no gain following an ambiguous gamble is larger than this difference following a risky gamble. We also tested whether the effects observed in the whole-brain ANOVA on reward outcomes in the MPFC were associated with age, by extracting the parameter estimates of this ROI for the difference scores and correlating these with age. No significant relations were observed (all *p's* > .1).

Table 2. MNI coordinates of Local Maxima Activated for the contrasts Risk Gamble > Ambiguity Gamble, and the reversed contrast.

	MNI coordinates					
Area of activation	x	y	z	T	pFWE	Volume
Risk Gamble > Ambiguity Gamble						
R middle occipital gyrus, including bilateral parietal lobe, bilat. temporal gyrus, bilat. postcentral gyrus	33	-85	16	17.32	< .001	9196
L calcarine gyrus	0	-85	1	15.43		
R calcarine gyrus	12	-91	4	14.65		
R precental gyrus	48	5	31	8.96	< .001	302
R middle frontal gyrus	27	-4	52	7.22	< .001	217
R superior frontal gyrus	24	2	70	3.32		
R inferior frontal gyrus (pars triangularis)	51	38	13	6.04	< .001	235
R inferior frontal gyrus (pars triangularis)	45	41	1	4.21		
Ambiguity Gamble > Risk Gamble						
R angular gyrus	57	-67	34	7.25	< .001	307
L angular gyrus	-42	-64	31	4.09	< .001	346
R rolandic operculum, including R superior temporal gyrus, R postcentral gyrus, R posterior insula	54	-19	16	5.00	< .001	206
R rolandic operculum	45	-19	16	4.85		
R superior temporal gyrus	60	-10	-5	4.00		
R precuneus	3	-55	34	4.89	< .001	202
L middle cingulate cortex	-12	-49	37	4.67		
L middle temporal gyrus	-69	-40	-2	4.33	.025	81
L middle temporal gyrus	-63	-28	-2	3.84		
L middle frontal gyrus, including L superior frontal gyrus	-30	20	49	4.47	< .001	177
	-36	11	58	3.90		
	-21	29	52	3.60		

Note: L = left; R = right; bilat = bilateral. Anatomical labels are based on the Automated Anatomical Labeling (AAL) atlas. Results were FWE cluster-corrected (p < .05).

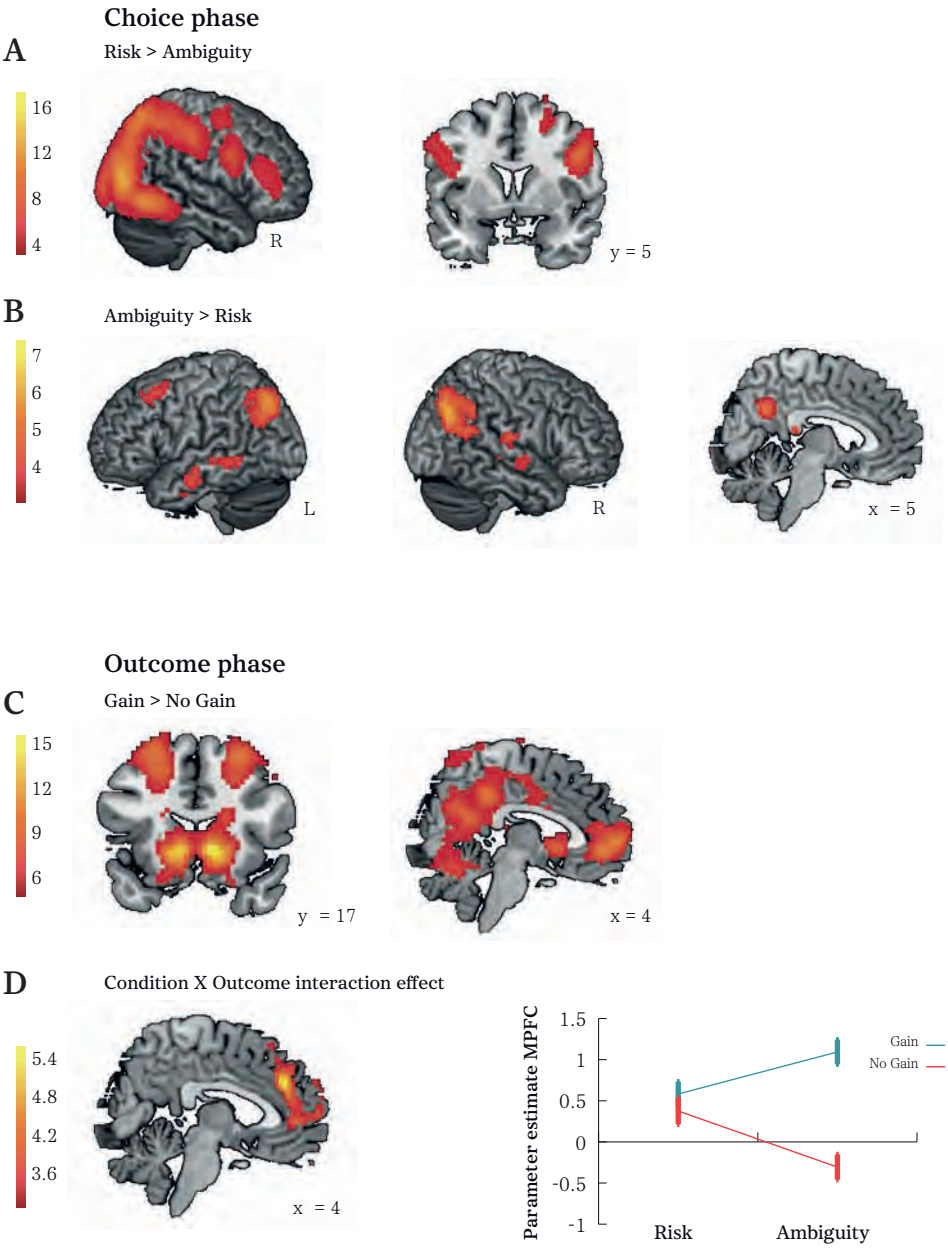

Figure 3. *Activation during the contrasts* ***A.*** *Risk Gamble > Ambiguity Gamble,* ***B.*** *Ambiguity Gamble > Risk Gamble,* ***C.*** *Gain > No Gain.* ***D.*** *Activation from the Condition * Outcome interaction effect. The graph is for illustrative purposes only.*

Table 4. MNI coordinates of Local Maxima Activated for the contrast Gain > No Gain , irrespective of risk and ambiguity

	MNI coordinates					
Area of activation	x	y	z	T	pFWE	Volume
Gain > No Gain, voxel-corrected						
R caudate nucleus	12	17	-5	15.51	< .001	11259
L caudate nucleus	-9	17	-5	13.73		
L anterior cingulate cortex, including bilat. superior medial gyrus, R mid orbital gyrus, bilat. middle frontal gyrus, bilat. precuneus	-6	44	1	10.83		
L inferior gyrus, including L superior temporal gyrus	-54	-49	-11	7.68	< .001	664
L middle temporal gyrus	-63	-7	-17	6.96		
L inferior temporal gyrus	-60	-58	-11	6.75		
R angular gyrus	42	-73	40	7.12	< .001	230
R angular gyrus	39	-67	55	5.82		
R superior parietal lobe	33	-76	52	5.30		
R superior temporal gyrus, including R fusiform gyrus	63	-4	1	7.02	< .001	556
R middle temporal gyrus	63	-4	-23	6.92		
R superior temporal gyrus	66	-4	-8	6.74		
R putamen	30	-13	7	5.97	< .001	58
L precentral gyrus	-48	2	22	5.55	.001	24
*Interaction effect Condition * Outcome, cluster-corrected*						
L superior medial gyrus, including R superior medial gyrus, R superior frontal gyrus, R anterior cingulate cortex	3	38	31	5.59	< .001	536
R superior frontal gyrus	18	50	40	4.38		
R middle frontal gyrus	21	59	28	4.19		
R inferior parietal lobule	45	-52	46	4.43	.001	115

*Note: L = left; R = right; bilat = bilateral. Anatomical labels are based on the Automated Anatomical Labeling (AAL) atlas. (FWE voxel-corrected, p < .05 and presented here with k >10) and the interaction effect of condition (risk, ambiguity) * reward outcome (Gain, No Gain; FWE cluster-corrected, p < .05).*

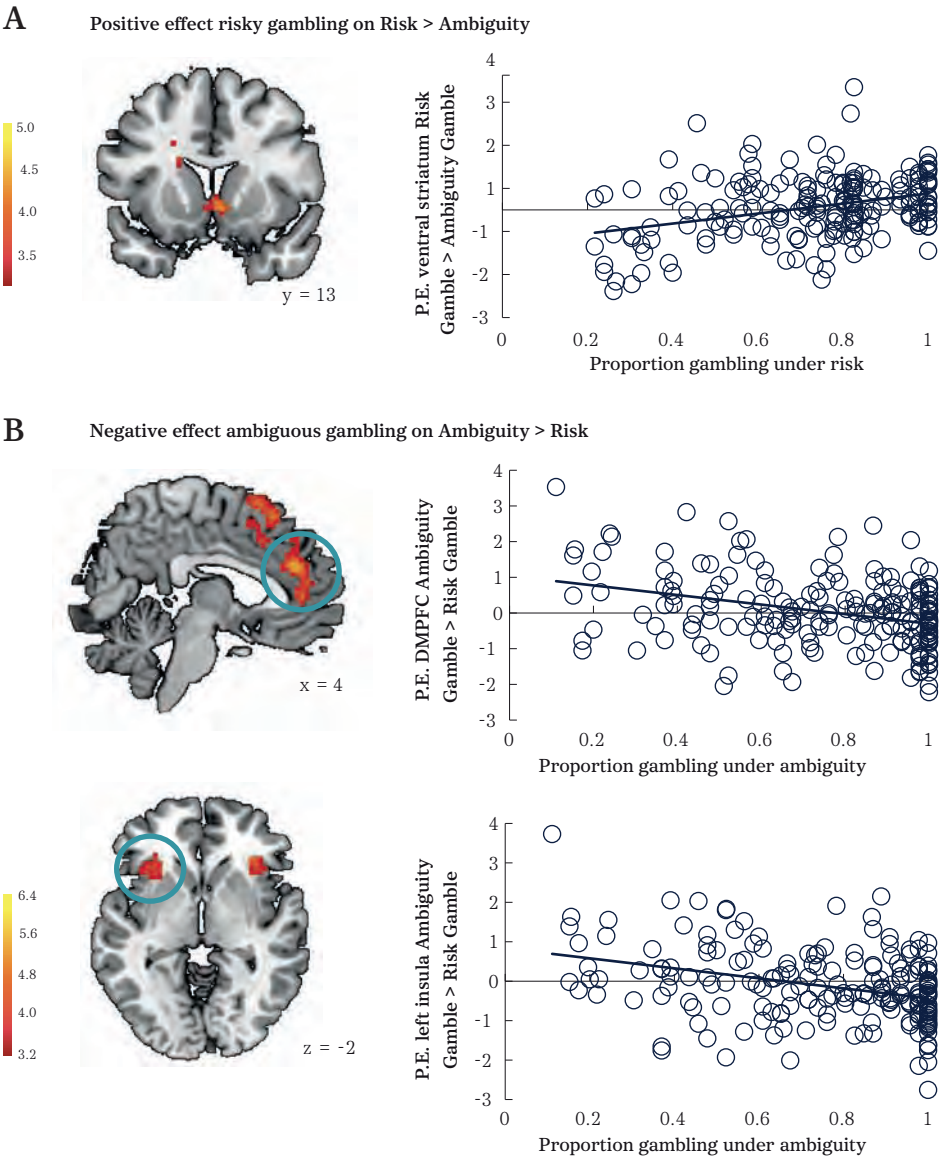

Figure 4. A. *The positive effect of risky gambling on Risk Gamble > Ambiguity Gamble in the ventral striatum. A higher frequency of gambling under risk was associated with increased ventral striatum activation during Risk Gamble > Ambiguity Gamble.* ***B.*** *The negative effect of ambiguous gambling on Ambiguity Gamble > Risk Gamble. Increased gambling behavior under ambiguity was associated with an attenuated DMPFC and bilateral insula response. The graphs are for illustrative purposes only. P.E. = parameter estimate.*

Table 5. MNI coordinates of Local Maxima Activated for the results of regressions with gambling behavior on Risk Gamble > Ambiguity Gamble and the reversed contrast.

	MNI coordinates					
Area of activation	x	y	z	T	pFWE	Volume
Positive effect of risky gambling on Risk Gamble > Ambiguity Gamble						
L caudate nucleus	-15	2	25	4.86	< .001	170
R caudate nucleus	6	14	-5	4.15	.008	105
Negative effect of ambiguous gambling on Ambiguity Gamble > Risk Gamble						
L anterior cingulate cortex	-9	35	19	6.44	< .001	429
R anterior cingulate cortex	6	38	25	5.38		
L superior medial gyrus	-9	32	31	5.06		
L supplementary motor area, including R supplementary motor area, bilat. superior medial gyrus, bilat. superior frontal gyrus, R middle cingulate cortex	-9	11	52	5.13	< .001	392
	-3	26	52	5.11		
	0	17	64	4.56		
L insula lobe	-27	26	4	4.88	.005	116
L insula lobe	-30	11	-14	4.49		
L insula lobe	-30	20	-11	4.32		
L inferior frontal gyrus (pars orbitalis)	-36	26	-5	3.53		
R insula lobe	33	29	-2	4.62	.005	117
R inferior frontal gyrus (pars orbitalis)	39	20	-20	3.93		
R inferior frontal gyrus (pars orbitalis)	42	29	-17	3.46		

Note: L = left; R = right; bilat = bilateral. Anatomical labels are based on the Automated Anatomical Labeling (AAL) atlas. Results were FWE cluster-corrected (p < .05).

Associations with individual-differences measures

Regressions with task behavior: Choice phase - Our main interest was to examine relations between brain activation during risky and ambiguous decision-making and individual differences in risk-taking tendencies. First we examined whether individual differences in gambling behavior in the wheel of fortune task were associated with different activation patterns during risky and ambiguous gambling, respectively. We observed a positive effect of risky gambling on the Risk Gamble > Ambiguity Gamble contrast in the VS (Figure 4A, Table 5). That is, participants

who gambled more frequently on risky trials (controlling for gambling in ambiguous trials) showed greater activation in this region during risk compared with ambiguity (Figure 4A, right panel).

In the reversed contrast (Ambiguity Gamble > Risk Gamble), we observed a negative effect of ambiguous gambling (controlled for risky gambling) in bilateral insula, DMPFC, and dorsal ACC/SMA (Figure 4B, Table 5). Specifically, these analyses show that participants who gambled less frequently on ambiguous trials in general, showed greater activation in these regions for Ambiguity Gamble > Risk Gamble when choosing to gamble (Figure 4B, right panel).

When we included age as an additional covariate in these analyses, these effects remained the same.

Table 6. MNI coordinates of Local Maxima Activated for the negative effect of ambiguous gambling on Gain > No Gain.

	MNI coordinates					
Area of activation	x	y	z	T	pFWE	Volume
L superior temporal gyrus, L posterior insula	-54	-19	13	4.74	< .001	531
L postcentral gyrus	-54	-13	40	4.44		
R superior frontal gyrus	24	20	58	5.67	.007	102
R middle frontal gyrus	45	26	37	3.82		
R middle frontal gyrus	42	35	43	3.65		
R precentral gyrus, including R supplementary motor area, R postcentral gyrus	39	-19	58	4.73	< .001	505
R paracentral lobule	3	-31	58	4.33		
R posterior insula lobe, including R superior temporal gyrus, R precentral gyrus, R postcentral gyrus, R inferior frontal gyrus (pars opercularis).	36	-7	13	4.26	< .001	244
R rolandic operculum	45	-7	19	4.25		
R rolandic operculum	48	-16	13	4.17		

Note: L = left; R = right; bilat = bilateral. Anatomical labels are based on the Automated Anatomical Labeling (AAL) atlas. Results were FWE cluster-corrected (p < .05).

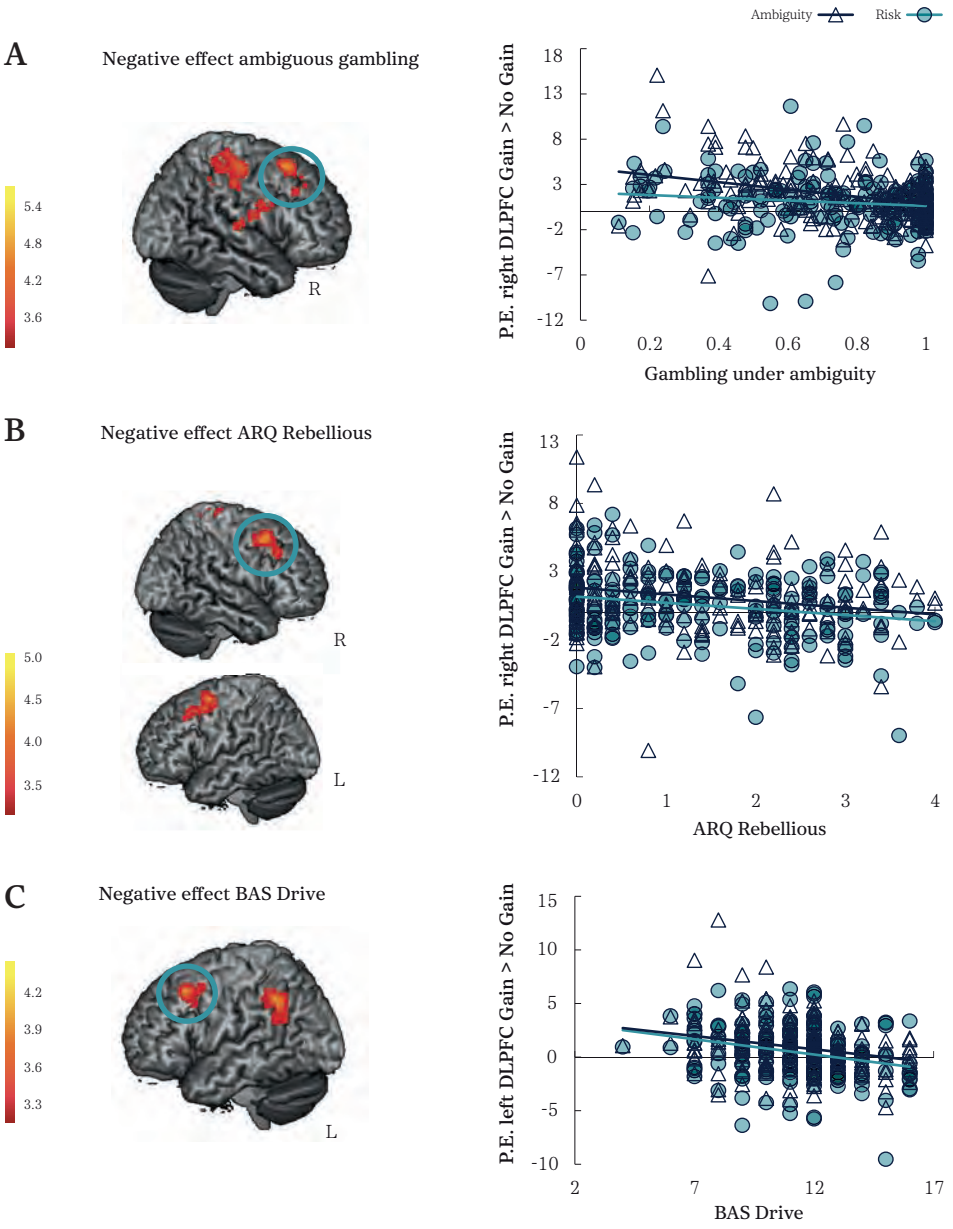

Figure 5. A. *The negative effect of gambling under ambiguity on Gain > No Gain.* ***B.*** *The negative effect of ARQ Rebellious behavior on Gain > No Gain.* ***C.*** *The negative effect of BAS Drive on Gain > No Gain. Activation was similar for both conditions (see graphs, right panels). P.E. = parameter estimate.*

Regressions with task behavior: Outcome phase - Similarly, as for the choice phase, we investigated effects of gambling in the wheel of fortune task on the reward outcome phase (Gain > No Gain, collapsed across risky and ambiguous conditions). A whole-brain regression with risky and ambiguous gambling behavior as predictors showed a specific negative effect of ambiguous gambling in the right DLPFC and right superior temporal gyrus (extending into the posterior insula; Figure 5A, Table 6). These effects remain the same when including age as an additional covariate.

We used an ROI approach to test whether the DLPFC activation differed between reward outcome processing following a risky or an ambiguous gamble. This was not the case: the partial correlations between ambiguous gambling (controlling for risky gambling) and DLPFC did not differ significantly between reward processing following risk or ambiguity (Fisher's Z = 1.35, p = .17; Ambiguity Gain > Ambiguity No Gain: r = -.302, p < .001; Risk Gain > Risk No Gain: r = -.183, p = .01). This result indicates that those participants who gambled less frequently in the ambiguous trials showed greater activation in this region when processing rewards, but this was not driven by processing rewards after risk or ambiguity (Figure 5A, right panel).

Regressions with self-reported risk-taking behavior: Choice phase - To test which regions were associated with self-reported risk-taking measures, we included ARQ and BIS/BAS subscales in a whole-brain regression. No activation in hypothesized

Table 7. MNI coordinates of Local Maxima Activated for the results of regressions with ARQ and BIS/BAS subscales on Ambiguity Gamble > Risk Gamble.

	MNI coordinates					
Area of activation	x	y	z	T	pFWE	Volume
Positive effect of BAS Drive on Ambiguity Gamble > Risk Gamble						
R inferior parietal lobe	54	-52	46	4.18	.02	70
Positive effect of BAS Fun Seeking on Ambiguity Gamble > Risk Gamble						
R supramarginal gyrus, including R postcentral gyrus	63	-28	49	3.87	.048	56
R supramarginal gyrus	51	-31	40	3.58		
R supramarginal gyrus	54	-34	49	3.51		

Note: L = left; R = right; bilat = bilateral. Anatomical labels are based on the Automated Anatomical Labeling (AAL) atlas. Results were FWE cluster-corrected (p < .05).

regions was observed during the choice phase (Risk Gamble > Ambiguity Gamble or vice versa). The only clusters that survived thresholding was a positive relation with BAS Drive and BAS Fun Seeking in parietal and motor brain regions during Ambiguity Gamble > Risk Gamble (summarized in Table 7). When including age as an additional covariate, only the effect of BAS Drive survived cluster correction.

Regressions with self-reported risk-taking behavior: Outcome phase - A similar regression was performed testing for effects of ARQ and BIS/BAS subscales on the general contrast Gain > No Gain. First, we observed a negative effect of ARQ Rebellious behavior in the bilateral DLPFC (Figure 5B; Table 8). Specifically, this

Table 8. MNI coordinates of Local Maxima Activated for the results of the regression with ARQ and BIS/BAS subscales on Gain > No Gain.

	MNI coordinates					
Area of activation	x	y	z	T	pFWE	Volume
Negative effect of ARQ Rebellious on Gain > No Gain						
R middle frontal gyrus	39	14	52	5.02	.006	112
R middle fro ntal gyrus	39	26	37	3.93		
L precental gyrus	-36	2	61	4.41	.001	148
L middle frontal gyrus	-36	5	52	4.25		
L middle frontal gyrus	-27	14	43	3.89		
R paracentral lobule	6	-34	73	4.06	.025	80
R precuneus	6	-46	67	3.82		
R precentral gyrus	15	-22	64	3.56		
Negative effect of BAS Drive on Gain > No Gain						
L inferior parietal lobule	-57	-52	40	4.45	.006	110
L angular gyrus	-42	-55	25	3.62		
L supramarginal gyrus	-60	-52	28	3.56		
L middle frontal gyrus	-42	23	49	4.43	.022	83
L middle frontal gyrus	-39	11	49	3.47		
L middle frontal gyrus	-33	20	43	3.46		

Note: L = left; R = right; bilat = bilateral. Anatomical labels are based on the Automated Anatomical Labeling (AAL) atlas. Results were FWE cluster-corrected ($p < .05$).

indicates that those participants who show more rebellious behavior in daily life, showed significantly less activation in the DLPFC when processing reward outcomes. Similar, but less pronounced, results were observed when including age as a covariate.

We tested whether this activation pattern was driven by outcome processing in the risky or ambiguous condition. When comparing the partial correlations between Rebellious behavior (controlling for the other ARQ and BIS/BAS subscales) and DLPFC activation in the risky, with the ambiguous condition, we observed no significant differences between these conditions (left DLPFC: Fisher's $Z = .72$, $p = .47$, right DLPFC: $Z = .06$, $p = .95$; ambiguity: left DLPFC $r = -.307$, $p < .001$, right DLPFC: $r = -.258$, $p = .001$, risk: left DLPFC: $r = -.239$, $p = .002$, right DLPFC: $r = -.252$, $p = .001$; Figure 5B, right panel). This shows that the negative association between rebellious behavior and reward outcome processing did not depend on whether the reward was preceded by a risky or ambiguous gamble.

With respect to BAS Drive, a greater tendency to work for rewards was also associated with an attenuated left DLPFC response when processing rewards (Figure 5C, Table 8). These effects remained the same when including age as an additional covariate.

Again we tested whether this activation pattern was driven by outcome processing in the risky or ambiguous condition. Similar to the association with Rebellious behavior, we observed that the association with BAS Drive did not differ ($Z = -.104$ $p = .92$) between rewards following a risky ($r = -.243$, $p = .001$) and ambiguous gamble ($r = -.233$, $p = .002$, Figure 5C, right panel).

Discussion

This study investigated the neural mechanisms underlying individual differences in risk-taking tendencies during risky and ambiguous decision-making in a large adolescent sample with a wide age range (11-24 years). We specifically focused on two indices of risk taking: task-related (gambling under risk and ambiguity) and self-reported indices of risk taking (the frequency of engaging in real-life risky behaviors and trait reward sensitivity). The analyses resulted in a number of main findings. First, we discovered that risky versus ambiguous gambling are reflected in different patterns of brain activation. Second, individual differences in task-related risk taking recruited different regions depending on whether the context was risky or ambiguous. Finally, individual differences in self-reported risk taking were primarily reflected in activation during reward outcome processing. The discussion is organized alongside these main findings.

Neural mechanisms underlying risky and ambiguous decision-making

First, we investigated the neural correlates of gambling and reward processing under risk and ambiguity, using a previously validated fMRI gambling paradigm (Blankenstein et al., 2017). Previous neuroimaging studies in adults have questioned whether risk and ambiguity are reflected by the same underlying neural mechanisms, given that risk and ambiguity preferences may separately influence risk taking (Tversky & Kahneman, 1992). Although some have predominantly observed overlap in the neural correlates underlying valuation under risk and ambiguity (Blankenstein et al., 2017; Levy, Snell, Nelson, Rustichini, & Glimcher, 2010), others have observed distinct neural patterns between these decision contexts (Hsu et al., 2005; Huettel et al., 2006), which may particularly arise when including individuals' preferences for risk and ambiguity (Blankenstein et al., 2017). When contrasting risky and ambiguous gambling, we observed that risk resulted in greater activation in the right ventral LPFC, bilateral precentral gyrus, and parietal cortex, whereas ambiguity resulted in greater activation in left dorsal LPFC and temporal lobe. Activation in the former set of regions may possibly serve the executive processing of explicit probabilities presented during risky trials as found in prior studies with adults (Blankenstein et al., 2017; Huettel, Song, & McCarthy, 2005; Huettel et al., 2006), but do not concur with adult findings of risk preferences in the striatum or OFC (Blankenstein et al., 2017; Engelmann & Tamir, 2009; Hsu et al., 2005). The regions that were particularly activated during gambling under ambiguity fit well with earlier findings of ambiguity coding in the LPFC in adults (Huettel et al., 2006).

We further addressed whether outcomes were processed differently after gambling in a risky or ambiguous context. Although VS and MPFC were generally activated in response to rewards irrespective of a risky or ambiguous decision context, a more dorsal region of the MPFC was particularly activated during rewards following ambiguous, compared with risky, gambles. A similar pattern has been observed in prior work with adults (although slightly more dorsal; Blankenstein et al., 2017), and was interpreted as a general signal of uncertainty coding, being particularly present in ambiguous contexts (based on a search in NeuroSynth, an online meta-analysis database; Yarkoni, Poldrack, Nichols, Van Essen, & Wager, 2011). Alternatively, the MPFC has been implicated in performance monitoring and feedback integration following risky decisions (McCormick & Telzer, 2017a; van Noordt & Segalowitz, 2012; Xue et al., 2009), which would concur with a learning signal over time that is greater in ambiguous compared to risky contexts. Although behavior did not change profoundly in both decision contexts, gambling increased slightly over time for ambiguous trials. Future studies may therefore further investigate the role of the MPFC in learning (e.g., behavioral adjustment) versus

resolving outcome uncertainty under risky and ambiguous conditions, for instance by using a paradigm in which outcomes influence subsequent decisions in a learning context, and using varying levels of ambiguity.

Relations with task-related and self-reported risk taking

Our main interest was to relate individual differences in risk-taking tendencies to brain activation during risky and ambiguous decision-making during adolescence, given that this is a time marked by a rise in risk taking (Steinberg, 2008). To this end we included participants from a wide age range, in which individual differences in risk-taking tendencies are most prominent (Bjork & Pardini, 2015; Willoughby et al., 2013). Although participants were encouraged to gamble by presenting gambling options higher in expected value than the safe option, there was substantial variability in risky and ambiguous gambling behavior, allowing the investigation of these individual-difference measures in relation to brain activity.

First, during the choice phase, a higher frequency of gambling under risk (but not ambiguity) was associated with increased activation in the VS in the risky condition only, whereas a greater tendency to gamble under ambiguity (but not risk) was related to reduced DMPFC and insula activation in the ambiguous condition only. Generally, we replicated prior research showing that enhanced risk taking is associated with greater striatum activation (Galvan et al., 2007), and reduced DMPFC and insula activation (Van Duijvenvoorde et al., 2015; Van Leijenhorst et al., 2010). However, we now show that these neural correlates differed across task conditions. Speculatively, these findings may relate to the difference in subjective evaluation of the decisions at hand, in which the tendency to engage in risky gambles may be triggered by a greater reward valuation, whereas the tendency to engage in ambiguous gambles is mainly driven by an aversion to uncertainty. Previous research has related insula and DMPFC activation in the context of risky decision-making as an affective and cognitive component (respectively) of uncertainty processing (Mohr, Biele, & Heekeren, 2010; Van Duijvenvoorde et al., 2015). That is, activation in the insula may reflect the increased experienced negative affect when encountering uncertainty (Van Duijvenvoorde et al., 2015), which may be more pronounced under ambiguity than risk. Simultaneously, activation in the DMPFC may function as a cognitive warning signal to prevent risky behavior and has been related to participants' subjective experience of uncertainty (Xue et al., 2009). This interpretation fits well with the finding that insula activation was heightened for those individuals who gambled less frequently in this condition.

A new direction in this study is that we related individual differences in risk-taking tendencies not only to choice, but also to outcome processing. We observed

that a greater tendency to gamble under ambiguity was associated with decreased right DLPFC activation during reward processing. In addition, greater self-reported rebellious behavior, and a greater drive for rewards, were also associated with a reduced DLPFC response when processing rewards. This contradicts prior research on adolescent individual differences in real-life risk taking and brain activation, which showed the opposite relation (a greater DLPFC response with increased risk taking; Qu et al., 2015), but is in line with prior research in young adults (Gianotti et al., 2009) and with studies that relate lower impulsivity to strengthened connectivity between the striatum and DLPFC (Achterberg, Peper, van Duijvenvoorde, Mandl, & Crone, 2016; Dixon, 2015; van den Bos, Rodriguez, Schweitzer, & McClure, 2014). These findings point towards an important role for the LPFC in individuals' risk preferences, and concurs with the idea that lower self-control in response to rewards may lead adolescents to engage in greater risk taking. However, it should be noted that in the current task, risk taking could be seen as advantageous (i.e., the gamble presented a higher expected value), thus leading to more monetary gains. Similarly, it may be adaptive to display certain levels of reward motivation or rebellious behavior, particularly in this age range (Romer, Reyna, & Satterthwaite, 2017). The adaptive nature of risk taking should be further examined, considering adolescence as a period of opportunities, and not only of risk (Crone, Duijvenvoorde, & Peper, 2016).

Limitations and future directions

A number of limitations need to be considered. First, although the current study included a wide age range across adolescence (11-24 years, an age range in which individual differences in daily-life risk taking are prominent; Bjork & Pardini, 2015; Willoughby, Good, Adachi, Hamza, & Tavernier, 2013), the majority of our findings were independent of age, except for the results on self-report measures. That is, ARQ and BAS subscales increased with age and/or peaked in adolescence, which is consistent with prior reports on these measures which is consistent with prior reports on these measures (Blankenstein et al., 2016; Urošević, Collins, Muetzel, Lim, & Luciana, 2012) and with previous reports of this sample (regarding the BAS scales, Braams et al. 2015; Schreuders et al., 2018). While in the current study we focused particularly on individual differences in an adolescent sample, it is surprising that we did not find effects of age on our neural results. Prior studies reported heightened activation in dorsal ACC in early adolescence (Van Leijenhorst et al., 2010) and in DMPFC, anterior insula, and subcallosal cortex in mid-adolescence with increasing risk processing (Van Duijvenvoorde et al., 2015; Van Leijenhorst et al., 2010) and adolescent peaks in striatum activity (Braams et al., 2015; Van Leijenhorst et al., 2010; Silverman, Jedd, & Luciana, 2015). Others reported a monotonic increase from

childhood to adulthood in MPFC during reward processing (Van Duijvenvoorde et al., 2015). Importantly, these studies included participants from late childhood/early adolescence (8-10 years), whereas our youngest participants were 11-12 years old. Indeed, in a recent review it was argued that information from childhood is needed to fully understand developmental patterns and underlying factors of risk taking across adolescence (Li, 2017). Furthermore, developmental effects are often not observed when the risky option is obviously advantageous (Defoe, Dubas, Figner, & Van Aken, 2015; Li, 2017), as in the current study. An opportunity for future research may therefore be to determine age effects in risk and ambiguity sensitivity, a question that may be tackled with paradigms including a non-safe alternative (e.g., Defoe et al., 2015) as well as including multiple levels of risk and ambiguity (Blankenstein et al., 2016) in a broad age range starting in late childhood and extending into adulthood.

Second, task behavior was not correlated to any of our measures on real-life risk taking. Studies using both task-related and self-report measures of risk taking often do not find significant correlations, which have been suggested to be caused by underpowered studies (for a review, see Sherman et al., 2017). However, the current study, and others (e.g., Mamerow, Frey, & Mata, 2016) with relatively large sample sizes also did not find associations between task-related and self-reported risk taking. Recently, a large comprehensive study with adults used a psychometric approach to examine the multidimensionality of risk taking (Frey, et al., 2017). This study showed that risk propensity measures (i.e., self-report measures on for instance sensation-seeking and impulsivity) and risk frequency measures (i.e., real-life risk behaviors such as smoking) were only weakly correlated with behavioral measures (i.e., revealed preferences: task-based risk measures such as behavior on the Balloon Analogue Risk Task and the Columbia Card Task). That is, the authors discovered that a general factor of risk preference emerged from the propensity measures and frequency measures, which did not share variance with behavioral measures (revealed preferences). Possibly, in the current study, task-related risk taking (a behavioral measure) and self-reported risk taking as measured with the BIS/BAS subscales (a propensity measure), and the ARQ subscales (a frequency measure) also reflect different behavioral manifestations of risk behavior in our adolescent sample. Although the psychometric properties of risk preferences in adolescence warrants further study, this echoes the need for and potential of including multidimensional measures of risk taking (i.e., behavior, propensity, and real-life frequencies) in adolescence.

Third, task behavior was heavily tuned towards gambling, by presenting participants with gambles much higher in expected value than the safe option. To derive a more sensitive measure of individuals' preferences for risk and ambiguity, future research may benefit from including an additional task that presents multiple

levels of risk and ambiguity (Blankenstein et al., 2017; Engelmann & Tamir, 2009).

Fourth, participants' gambling frequency determined the number of gain and no gain trials included in the analyses. That is, those participants who gambled more frequently experienced more reward outcomes than those participants who chose the safe option more frequently, which may have biased our results in the reward outcome phase. However, a loss of power due to fewer trials is unlikely to drive our main results, given that less gambling actually led to greater activation during choice and outcome.

Finally, indices of real-life risk taking were based on retrospective, self-report questionnaires. An opportunity for future research is to more explicitly measure day-to-day risk taking, for instance by using ecological momentary assessments, in which participants are asked to answer questions multiple times each day for an extended period of time, making it possible to collect rich, real-time data on individuals' risk-taking behavior (Shiffman, Stone, & Hufford, 2008; Turner, Mermelstein, & Flay, 2004).

Conclusion

This study is the first to examine individual differences in risk taking in adolescence in relation to the neural mechanisms underlying decision-making under risk and ambiguity. Using a previously established fMRI gambling paradigm, we were able to study gambling and reward processing under risk and ambiguity in a large adolescent sample spanning a wide age range (11-24 years). We demonstrate that risky and ambiguous gambling is reflected in different patterns of brain activation, and that the MPFC appears key in processing reward outcomes following ambiguity. In addition, individual differences in task-related and self-reported risk-taking tendencies were associated with activation in the VS, LPFC, insula and DMPFC, regions previously associated, respectively, with reward processing, cognitive control, and cognitive-affective integration. Moreover, we found that the neural mechanisms underlying task-related risk taking were differentially recruited depending on whether the choice context was risky or ambiguous. Finally, reward valuation in the LPFC seems key for individual differences in risk-taking tendencies in this adolescent sample. Together, this study demonstrates the importance of considering multiple measures of risk taking, and contextual moderators, in unraveling the neural mechanisms underlying risk taking in adolescents.

Supplementary materials

A1. Behavioral age effects

We explored linear, quadratic, and cubic changes with age (with age as a polynomial predictor) on the behavioral risk-taking measures using hierarchical multiple regression models. These regressions indicated that gambling under risk increased slightly with age (i.e., linearly: $R^2 = .03$, $F(1, 196) = 6.35$, $b_{age} = .014$, $p = .013$), whereas gambling under ambiguity did not ($b_{age} = .010$. $p = .126$). For the ARQ subscales, we observed no age effects for Thrill-seeking behavior ($p = .614$), a quadratic age effect for Rebellious behavior ($R^2 = .40$, $\Delta F(2, 189) = 6.73$, $\Delta p = .010$, $b_{age^2} = -.021$, $p_{age^2} = .019$), and positive linear age effects for Reckless ($R^2 = .26$, $F(1, 190) = 66.23$, $b_{age} = .099$, $p < .001$) and Antisocial behavior ($R^2 = .085$, $F(1, 190) = 17.67$, $b_{age} = .059$, $p < .001$). Finally, we observed a positive linear age effect for BAS Drive ($R^2 = .022$, $F(1, 180) = 3.98$, $b_{age} = .129$, $p = .048$), a quadratic age effect for BAS Fun seeking (peaking around 18-20 years, $R^2 = .06$, $\Delta F(2, 179) = 6.33$, $\Delta p = .013$, $b_{age^2} = -.039$, $p_{age^2} = .018$), no significant age-related change for BAS Reward responsiveness ($p = .182$), and a positive linear age effect for BIS ($R^2 = .023$, $F(1, 180) = 4.15$, $b_{age} = .211$, $p = .043$).

Table A1. MNI coordinates of Local Maxima Activated for the positive effect of age (linear) on Ambiguity Gamble > Risk Gamble.

	MNI coordinates					
Area of activation	x	y	z	T	pFWE	Volume
R superior parietal lobule	18	-58	49	4.77	.002	139
	15	-67	64	4.24		
	15	-61	58	4.14		

Note: L = left; R = right; bilat = bilateral. Anatomical labels are based on the Automated Anatomical Labeling (AAL) atlas. Results were FWE cluster-corrected (p < .05).

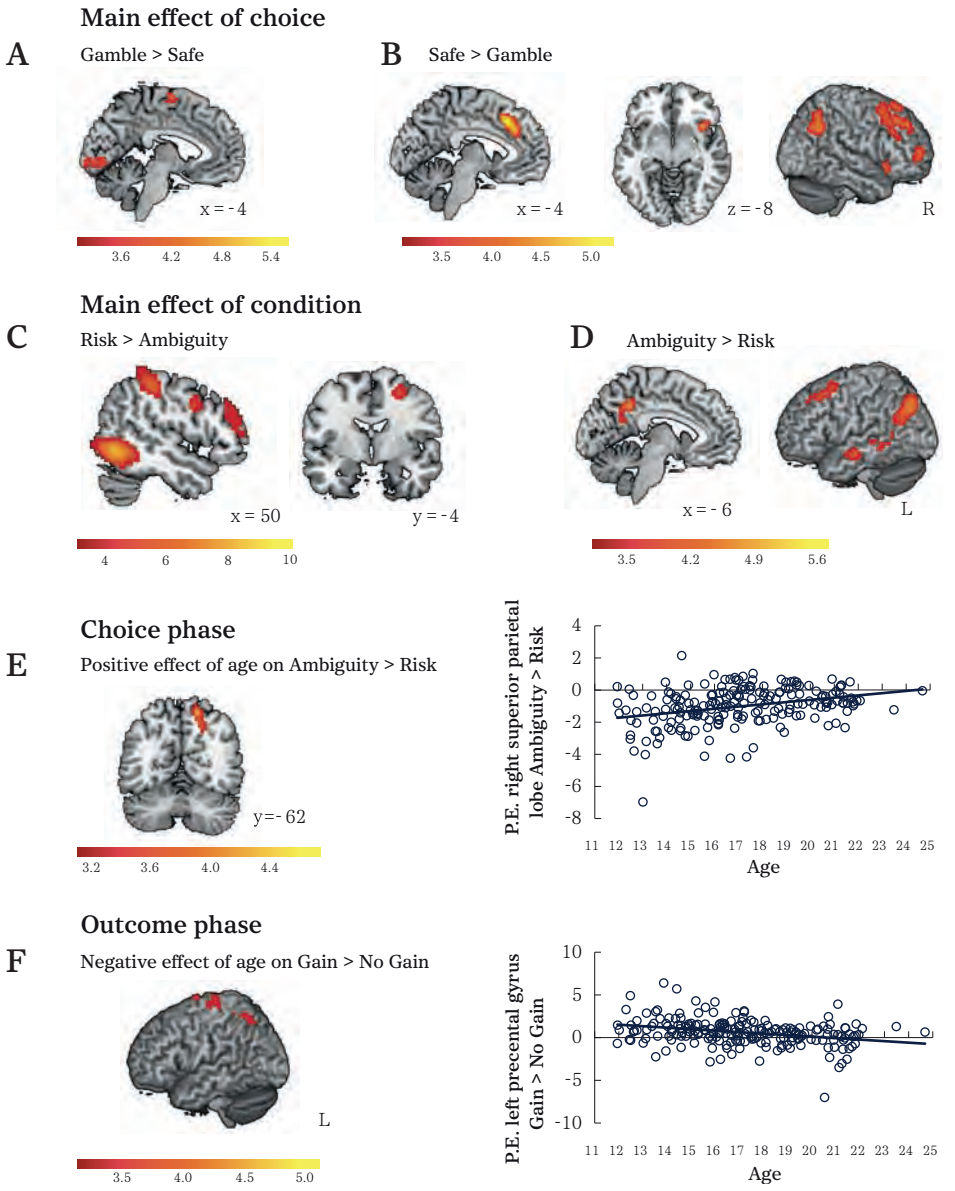

Figure A1. *Supplementary whole-brain results, FWE cluster-corrected ($p < .05$).* ***A-D.*** *Results of the choice (gamble, safe) * condition (risk, ambiguity) whole-brain ANOVA, showing the main effect of choice (**A.** Gamble > Safe and **B.** Safe > Gamble) and the main effect of condition (**C.** Risk > Ambiguity and **D.** Ambiguity > Risk). There was no interaction effect.* ***E.*** *The positive effect of age on Ambiguity Gamble > Risk Gamble.* ***F.*** *The negative effect of age on Gain > No Gain.*

A2. Gambling versus choosing safe across risk and ambiguity

Although not the main focus of the current study, we tested whether gambling versus choosing safe was coded differently for risk versus ambiguity. To this end we conducted a whole-brain choice (gamble, safe) * condition (risk, ambiguity) ANOVA. This analysis, including 152 participants (i.e., participants who chose the gamble and safe option in each condition), resulted in a main effect of choice, and a main effect of condition, but no interaction effect. This indicates that gambling versus choosing safe (and vice versa) was coded similarly for risk and ambiguity. The results of the main effects are shown in Table A2 and Figure A2 and described below.

The main effect of choice showed increased activation in the supplementary motor are for Gamble > Safe, and increased activation in anterior cingulate cortex, right ventrolateral and dorsolateral PFC, and right anterior insula for Safe > Gamble. With respect to the main effect of condition we observed heightened right lateralized DLPFC activation for Risk > Ambiguity (irrespective of the type of choice), and left lateralized DLPFC, and precuneus, activation for Ambiguity > Risk.

Table A2. MNI coordinates of Local Maxima Activated Clusters for results of the choice (gamble safe) * condition (risk, ambiguity) ANOVA.

		MNI coordinates					
Effect	Area of activation	x	y	z	T	pFWE	Volume
Gamble > Safe	L occipital middle gyrus	-15	-97	7	5.50	< .001	727
	R cuneus	21	-94	10	4.78		
	L supplementary motor area	-3	-7	67	4.08		85
Safe > Gamble	L superior medial gyrus	-3	23	43	5.19	< .001	262
	R anterior cingulate cortex	12	29	25	4.44		
	R superior frontal gyrus, including R superior medial gyrus	21	41	37	4.50	< .001	477
	R middle frontal gyrus	27	29	46	4.39		
	R middle frontal gyrus	42	26	34	4.13		
	R inferior parietal lobe	51	-58	46	4.45	< .001	211
	R angular gyrus	51	-61	37	4.45		
	L inferior parietal lobe	-48	-61	52	4.34	.014	78

Table A2. Continued

Effect	Area of activation	MNI coordinates			T	pFWE	Volume
		x	y	z			
Safe > Gamble (continued)	L inferior parietal lobe	-45	-58	43	3.85		
	R insula lobe	36	17	-8	4.31	.03	65
	R middle frontal gyrus	30	53	4	4.23	.003	106
	R superior frontal gyrus	18	62	7	3.44		
Risk > Ambiguity	R middle occipital gyrus	33	-85	10	10.08	< .001	5534
	R superior parietal lobe	21	-67	58	9.55		
	R inferior temporal gyrus	45	-67	-5	9.52		
	R precentral gyrus	48	5	31	5.16	.016	76
	R superior frontal gyrus	27	-4	55	4.82	.047	58
	R inferior frontal gyrus (pars Triangularis)	54	35	28	4.35	.019	73
	R middle frontal gyrus	54	41	19	3.95		
Ambiguity > Risk	L inferior parietal lobe	-45	-76	37	5.05	< .001	334
	L inferior parietal lobe	-39	-76	46	4.81		
	L angular gyrus	-51	-70	34	4.50		
	L middle frontal gyrus	-24	20	46	4.92	< .001	246
	L middle frontal gyrus	-33	11	58	3.93		
	L superior frontal gyrus	-18	38	28	3.92		
	R angular gyrus	57	-67	31	4.83	< .001	166
	R angular gyrus	63	-58	25	4.45		
	L precuneus	-9	-49	40	4.59	.001	127
	L precuneus	-3	-55	25	3.63		
	R precuneus	6	-55	22	3.33		
	L middle temporal gyrus	-51	-19	-14	4.21	.008	88
	L middle temporal gyrus	-57	-13	-8	4.15		

Note: L = left; R = right. Anatomical labels are based on the Automated Anatomical Labeling (AAL) atlas. Results were FWE cluster-corrected ($p < .05$).

Table A3. MNI coordinates of Local Maxima Activated for the negative effect of age (linear) on Gain > No Gain.

	MNI coordinates					
Area of activation	x	y	z	T	pFWE	Volume
Negative effect of age on Gain> No Gain, cluster-corrected						
L precentral gyrus, including L superior parietal lobe, L supplementary motor area, L precuneus	-21	-25	58	5.11	< .001	368
	-21	-25	67	4.73		
L postcentral gyrus	-21	-49	55	4.47		
R precentral gyrus, including R supplementary motor area	18	-25	67	4.63	< .001	167
R paracentral lobule	15	-28	58	4.38		
R superior frontal gyrus	15	-1	73	4.02		
R superior frontal gyrus	18	-7	70	3.87		

Note: L = left; R = right; bilat = bilateral. Anatomical labels are based on the Automated Anatomical Labeling (AAL) atlas. Results were FWE cluster-corrected (p < .05).